COMPDYN 2017
6th ECCOMAS Thematic Conference on
Computational Methods in Structural Dynamics and Earthquake Engineering
M. Papadrakakis, M. Fragiadakis (eds.)
Rhodes Island, Greece, 15–17 June 2017

MASS VARIATION WITH DISSIPATIVE STEEL STRUCTURES UNDER SEISMIC LOADS

P. Knoedel[1] **and T. Ummenhofer**[1]

[1] KIT Steel & Lightweight Structures
Research Centre for Steel, Timber and Masonry
Otto-Ammann-Platz 1, D-76131 Karlsruhe, Germany
peter.knoedel@kit.edu
thomas.ummenhofer@kit.edu

Keywords: plastic structures, seismic design, EC8, dissipation, viscous damping, time history, pushover, lateral force method, response spectrum.

Abstract. *In seismic engineering different levels of structural analysis are used, depending on complexity and importance of the structure and the required accuracy.*

- *Non linear time history analysis is used along with a full model of the structure to give the most accurate results. This method requires most effort and a well predesigned structure.*
- *Quasi static pushover analysis is used to get an insight of the subsequent development of plastic mechanisms under horizontal load patterns. This method requires only the modelling of the retaining system which, in the case of steel structures, could consist only of a pair of columns and the X-type braces in between.*
- *The simplest, but most inaccurate way, is to use the lateral force method (e.g. according to Eurocode 8), which can easily be handled by hand calculations. The dynamic behaviour of the structure is modelled as a single-degree-of-freedom oscillator and adopted to the real behaviour by a behaviour factor q.*

It is evident, that for predesigning purposes, the number of dissipative elements along with their performance must be adjusted depending on the total oscillating mass, so that the target displacements are met. However, in the respective design codes no rules are given on how to carry out this task. This holds as well for most of the scientific publications, which describe refined analyses for given structures, but do not provide guidance for predesign.

The present paper reports on a study on mass variation with a multi-storey steel structure. With a given dissipative structure a variation of the masses in each storey results – apart from a change in the natural frequency – in a different storey drift. This is becoming equivalent to a structure with given masses and variation of the performance of the dissipative elements, e.g. by altering the cross section of the braces. In the study a rule is developed, which describes the minimal required performance of the dissipative elements with a given mass and target storey drift. Thus, the structural engineer can adopt the bracing elements to the given needs.

1 TERMS AND ABBREVIATIONS

DAF	dynamic amplification factor, relates the response amplitude of the structure to the driving displacement amplitude
DBF	design by formulae (acronym given in EN 13445-3 Clause 5.2 [1])
PGA [m/s^2]	peak ground acceleration
SDOF	single degree of freedom (oscillator); simplest possible mass-spring-system
ζ	(zeta) damping ratio, see eq. 4; in German the term *Lehr*'sches Dämpfungsmaß D is paying tribute to *Ernst Lehr*, a material scientist and mechanical engineer; in EC8 [2] ξ (xi) is used, presumably due to mistaking ζ and ξ
ω [rad/s]	angular frequency

2 INTRODUCTION

When designing engineering structures, a balance is made of the effort which needs to be spent and the design result that wants to be achieved. E.g. with air- and spacecraft reduction of mass is extremely important, whereas design effort and money spent is only secondary. With most civil engineering structures, it's the other way round: expensive design hours need to be reduced, working hours in the shop and on site need to be reduced, whereas reduction of mass is only secondary. In seismic engineering it can be both: for simple structures and small or medium PGAs a simple and conservative design with hand-calculation rules can be sufficient. With complicated structures and medium or high PGAs sophisticated FEA such as time history simulation is needed.

Previously, the authors published some studies, where different levels of design methods were discussed [3], [4], [5]. Also, it was pointed out, which results can be achieved and how they can be verified [7], [8].

On the hand-calculation level (i.e. lateral force method), it seems to be sufficient, to assign the calculatory horizontal force to one or more bracing systems. On the resistance side, the assigned bracing systems counteract with their plastic capacity, e.g. plastic normal force with diagonal systems [3], plastic bending moments with frame systems [5] or plastic shear force with panel systems [10]. In some cases, separate devices are arranged, which are basically designed to provide a hysteretical behaviour [11], [12], [13]. For this cases it is interesting to find a simple predesign method in order to decide on the number of devices needed, before extensive FEA are started.

3 STATE OF THE ART

3.1 SDOF and viscous damping

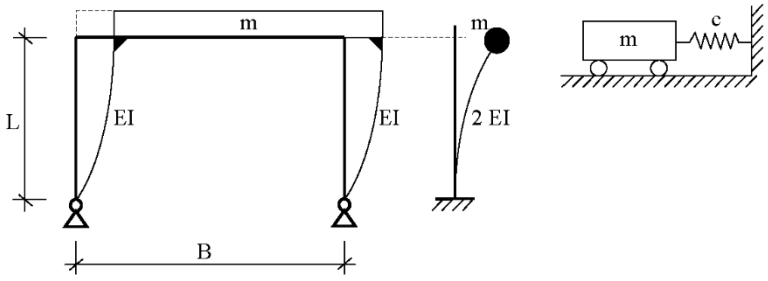

Fig. 1. Single storey frame arrangement and derived SDOF oscillator (taken from [4])

$$m \cdot \ddot{x} + d \cdot \dot{x} + c \cdot x = F(t) \tag{1}$$

$$x(t) = A \cdot e^{-\zeta \omega t} \cdot \sin(\omega \cdot \sqrt{1-\zeta^2} \cdot t) \tag{2}$$

Classical SDOF oscillators involve a mass inertia (first term in eq. 1), a viscous damping (second term in eq. 1) and an restoring force (third term in eq. 1) on the left hand side of the equal sign. On the right hand side an external load is given, which represents the "drive". Thus, the equation of motion is formulated as a quasi-static equilibrium condition of the aforementioned forces.

$$\omega = \sqrt{\frac{c}{m}}$$
$$f = \frac{\omega}{2\pi} = \frac{1}{2\pi}\sqrt{\frac{c}{m}} \tag{3}$$

The known solutions (eq. 2) provide information such as the angular frequency ω [rad/s] or the frequency f [1/s] and the period T, being the reciprocal value.

Increasing mass causes under-proportional increase of the fundamental period, see eq. 3. With respect to the lateral force method in seismic design, increasing mass causes proportional increase of the base shear. That is, if the fundamental response period is remaining on the plateau of the response spectrum. If the fundamental response period is bigger than the control period T_C (see fig. 3.1 in [2]), the branch of the response spectrum decreases. However, the decreased acceleration, multiplied by the increased mass, which caused the increased fundamental period, still leads to an increased base shear. Thus, increasing the mass in a structure with given stiffness, always will result in increasing base shear [14].

$$\zeta = \frac{d}{d_{crit}} \tag{4}$$

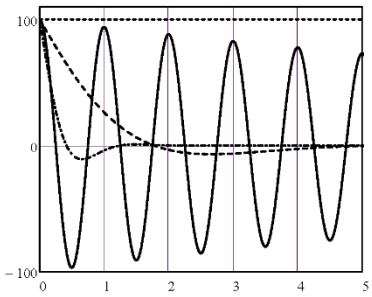

Fig. 2. Family of time-history curves of free, damped vibration with T = 1 s; governing parameter of the family of curves is ζ = 1.00; 0.99; 0.80; 0.01;

The damping constant d [N·s/m] is usually related to *critical damping* where oscillating motion changes into a creep motion (as it is given in most textbooks). From a mathematical point of view this is not true. Creep motion implies, that the motion approaches zero asymptotically, without changing the sign. Obviously, according to eq. 2, the sign change is not lost, but rather shifted to infinity, see Fig. 2. In eq. 2 the term $\sqrt{1-\zeta^2}$ can be regarded as *frequency correction* term. Other than the shock absorbers of a vehicle chassis, damping with building structures is rather low. According to EC1-1-4 informative Annex Table F.2, typical values of the *logarithmic decrement* for steel buildings may be assumed to be δ = 0.05, other metal structures such as slender chimneys or aluminium bridges may go down below δ = 0.02. By use of

$$\zeta = \frac{\delta}{2\pi} \tag{5}$$

these values transform to $\zeta = 0.008$ or $\zeta = 0.003$ and below. Even for a typical building according to EC8-1-1 [2], for which a value of $\zeta = 0.050$ may be assumed, the frequency correction term amounts to 0.9987. From this can be concluded, that for engineering purposes no correction of the natural frequency need to be taken into account.

In a forced harmonic motion, the steady-state amplitude is depending only on the damping ratio, so that

$$\mathrm{DAF} = \frac{1}{2\zeta} \tag{6}$$

This holds for force amplitudes as well as for relative displacements of oscillator and base in a base-displacement driven system [15].

Apart from damping, a non-linear spring c can also cause a limitation of amplitudes. The simplest possible formulation for this, where analytical solutions can be achieved, is the *Duffing* oscillator [16]. The restoring force is described as function of the third power of the displacement. Applications have been presented in [8].

3.2 Time history with plasticity

In a previous study, the authors used multi-storey frames to investigate the behaviour factors due to plastic response of the different structures [5].

Usually, in seismic design codes the base acceleration PGA is prescribed according to a local seismic zonal map. With time history simulations however, it is more convenient to have prescribed base displacement amplitudes. For harmonic motions, these can be derived by using the derivatives of the equation of harmonic motion

$$x = \mathrm{A} \sin \omega t \tag{7}$$

$$\ddot{x} = -\mathrm{A}\omega^2 \sin \omega t \tag{8}$$

We see from eq. 8, that we need to divide the acceleration amplitude by ω^2 in order to receive the displacement amplitude. For convenience we introduce

$$\omega = \frac{2\pi}{T} \tag{9}$$

and get

$$\mathrm{x}_{max} = \mathrm{a}_{max} \frac{T^2}{4\pi^2} \approx 0.0253 \cdot \mathrm{a}_{max} \cdot T^2 \tag{10}$$

For the below chosen seismic event (see section 3.3) and the fundamental period of the structure (see section 4) we receive

$$\mathrm{a}_{max} = \mathrm{a}_{gR} \cdot \gamma_I \cdot \mathrm{S} = 1.6 \frac{m}{s^2} \cdot 1.0 \cdot 1.5 = 2.4 \frac{m}{s^2} \tag{11}$$

$$\mathrm{x}_{max} = 2.4 \frac{m}{s^2} \cdot \frac{(1.6075\ \mathrm{s})^2}{4\pi^2} = 157\ \mathrm{mm} \tag{12}$$

Note, that this approach has been described in [4] eq. 23. Of course, using of a harmonic drive with reduced number of driving amplitudes is a gross simplification compared to real seismic records. On the other hand, according to Table 1 in [8] this is a necessary step back in order to be able to check the numerical results vs. known analytical evidence.

Real seismic data are given exemplary in Figures 3, 4 and 5, where the recorded ground accelerations and displacements, the respective spectra, and the response of different SDOF oscillators are given. The station code E-000182 is referring to a station, which has a distance

of only 12 km to the epicentre, so we are looking at a nearfield event (see Annex B.6 in [18]). As we stated in a previous paper [4] and can be seen in the time history plots in Fig. 3, there are only some few major peaks in design magnitude with near-field events. With far-field events the number of major peaks is much bigger, but the magnitude might be one order of magnitude lower. This might be seen as background information for the provision in EC8-1-1 3.2.3.1.2 (3), that steady state acceleration should be maintained for at least 10 seconds.

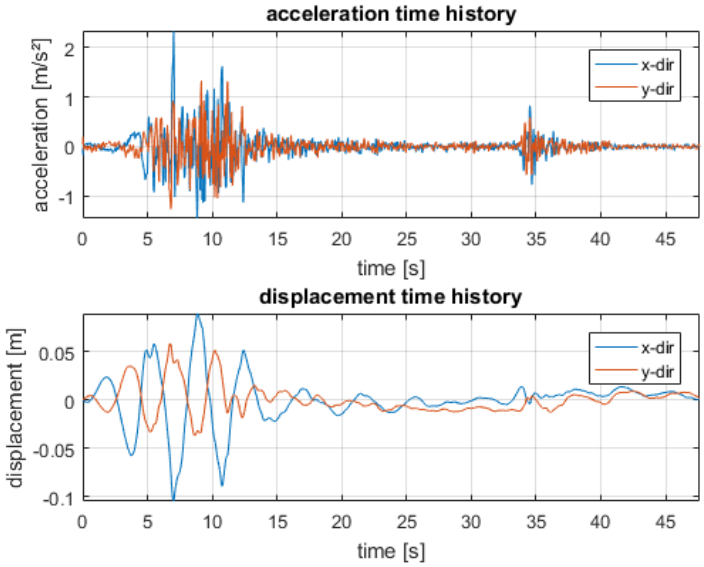

Fig. 3. Exemplary seismic data from Tabas Earthquake 16.09.1978 (E-000182 [18]) – acceleration and displacement time history

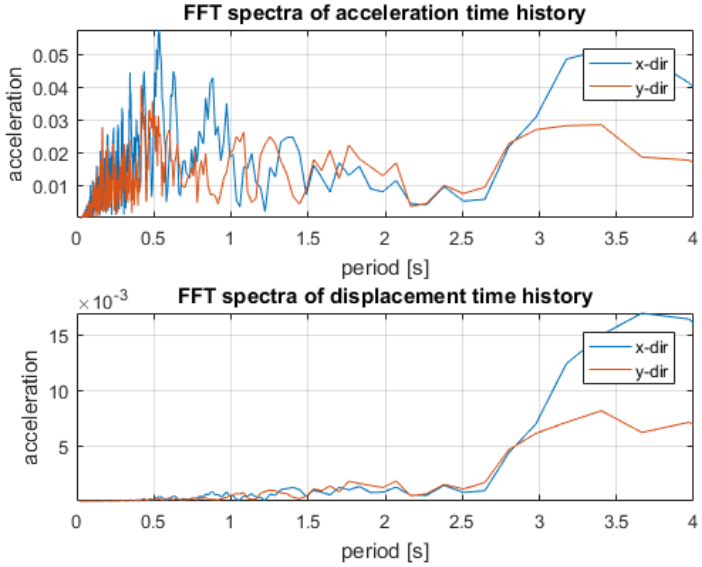

Fig. 4. Exemplary seismic data from Tabas Earthquake 16.09.1978 (E-000182 [18]) – acceleration and displacement periodal spetra

We can also see, that there is a big qualitative difference between the ground motion spectrum in Fig. 4 and the response spectrum of the structure in Fig. 5. This is sometimes mistaken, when artificial or recorded seismic data are scaled to the *response*-spectra in EC8 and then are

used as *input*-data for a FE time history calculation. If this is done, the DAF is used twice: first, a factor of 2.5 is used, which is implied in the response spectrum of EC8; second, the DAF of the actual modelled structure is (i.e. difference between input and output) is calculated via FEA.

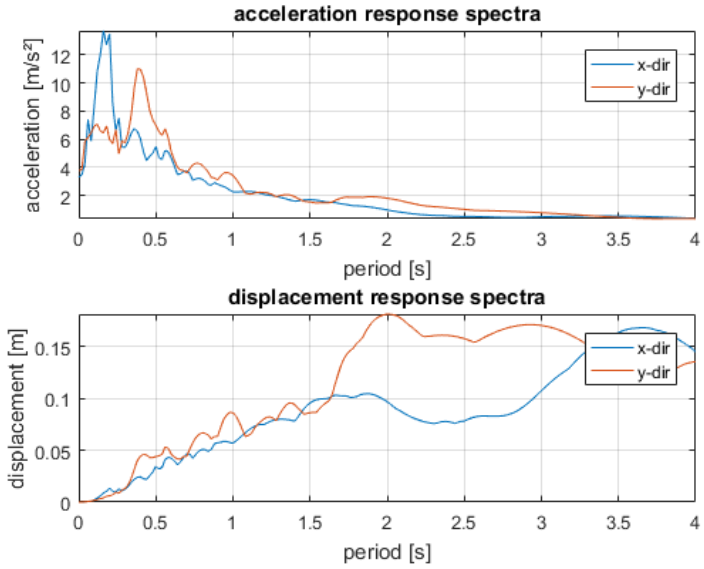

Fig. 5. Exemplary seismic data from Tabas Earthquake 16.09.1978 (E-000182 [18]) – acceleration and displacement periodal SDOF response spectra

3.3 Lateral Force Method (DBF)

In EC8 [2], the lateral force method is named in Clause 4.3.3.1 (3a), based on a modal response spectrum analysis, which is called "reference method for determining the seismic effects" in Clause 4.3.3.1 (2)P.

The lateral force method involves a linear structural analysis. The capability of the structure to dissipate energy and thus producing smaller response amplitudes, than a elastic structure would have, is captured by the behaviour factor q.

Following the basics of structural dynamics, we have (EC8 Clause 4.3.3.2.2 (1) eq. 4.5)

$$F_b = S_{d,hor} \cdot m \cdot \lambda \tag{13}$$

where

F_b [N]	base shear of the structure
$S_{d,hor}$ [m/s²]	effective horizontal acceleration
m [kgs]	oscillating mass of the structure
λ	correction factor, which will not be discussed in this paper (assuming λ= 1)

The effective acceleration is given by EC8 Clause 3.2.2.5 (4) eq. 3.14

$$S_{d,hor,max} = a_g \cdot S \cdot \frac{2.5}{q} \tag{14}$$

$$\text{where } a_g = a_{g,R} \cdot \gamma_I \tag{15}$$

$$S_{d,hor}(T) = S_{d,hor,max} \cdot \frac{T_C}{T} \quad \text{if } T_C \le T \le T_D \tag{16}$$

$$S_{d,hor}(T) = S_{d,hor,max} \cdot \frac{T_C \cdot T_D}{T^2} \quad \text{if } T_D \le T \tag{17}$$

$$S_{d,min} = \beta \cdot a_g \tag{18}$$

$S_{d,hor,max}$ [m/s^2] plateau value of the design response spectrum, independent of the period
a_g [m/s^2] design ground acceleration; eq. 15 is given in EC8 Clause 3.2.1 (3)
$a_{g,R}$ [m/s^2] reference PGA according to the relevant seismic zone map
γ_I importance factor; values are given in NOTE to EC8 Clause 4.2.5 (5)P; Importance Classes for buildings are defined in EC8 Table 4.3
S soil factor, given in EC8 Tables 3.2 and 3.3; for ground types see Table 3.1
2,5 DAF
q behaviour factor; EC8 Clause 6.1.2, (2)P and Table 6.1
T_B, T_C, T_D [s] control periods given in EC8 Tables 3.2 and 3.3, where T_B and T_C are limiting the plateau; for ground types see Table 3.1
(present choice: ground type C; spectrum type 2; 0.10; 0.25; 1.20)
$S_{d,hor}(T)$ [m/s^2] reduced acceleration, if the fundamental period exceeds T_C
β lower bound factor for the horizontal design spectrum; recommended to be 0.2, see NOTE after EC8 eq. 3.16

As we can see from the above equations, the base shear F_b is proportional to the mass. Thus, in a hand-calculation according to the lateral force method, a variation of mass would change the need for the strength of bracing elements proportional.

Following the example given in [4], but with 6 m span and 4 m height, we receive

$$S_{d,hor,max}(\mathrm{q}=1.5) = 1.6\frac{m}{s^2}\cdot 1.0\cdot 1.5\cdot\frac{2.5}{1.5} = 4.0\frac{m}{s^2} \tag{19}$$

$$S_{d,hor,max}(\mathrm{q}=4) = 1.6\frac{m}{s^2}\cdot 1.0\cdot 1.5\cdot\frac{2{,}5}{4} = 1.5\frac{m}{s^2} \tag{20}$$

Combining this with a storey mass of 72 000 kgs, we receive a plateau base shear of

$$F_b(\mathrm{q}=1.5) = 4.0\frac{m}{s^2}\cdot 72\,000\ \mathrm{kgs}\cdot 1.0 = 288\ \mathrm{kN} \tag{21}$$

$$F_b(\mathrm{q}=4) = 1.5\frac{m}{s^2}\cdot 72\,000\ \mathrm{kgs}\cdot 1.0 = 108\ \mathrm{kN} \tag{22}$$

As will be seen in the numerical study below, this configuration has a fundamental period of T = 1.61 s. Thus, we can reduce the calculatory acceleration by use of eq. 17 with a factor of

$$k = \frac{T_C\cdot T_D}{T^2} = \frac{0.25\ s\cdot 1.2\ s}{(1.61\ s)^2} = 0.12 \tag{23}$$

This gives a reduced base shear of

$$F_b(\mathrm{T};\ \mathrm{q}=1.5) = 288\ \mathrm{kN}\cdot 0.12 = 34.6\ \mathrm{kN} \tag{24}$$

$$F_b(\mathrm{T};\ \mathrm{q}=4) = 108\ \mathrm{kN}\cdot 0.12 = 13.0\ \mathrm{kN} \tag{25}$$

With the lower bound condition of eq. 18

$$F_{b,min} = \beta\cdot a_{g,R}\cdot\gamma_I\cdot \mathrm{m} = 0.2\cdot 1.6\frac{m}{s^2}\cdot 1.0\cdot 72\,000\ \mathrm{kgs} = 23.0\ \mathrm{kN} \tag{26}$$

we receive the final design base shear

$$F_b(\mathrm{T};\ \mathrm{q}=1.5) = 34.6\ \mathrm{kN} \tag{27}$$

$$F_b(\mathrm{T};\ \mathrm{q}=4) = 23.0\ \mathrm{kN} \tag{28}$$

Using the horizontal storey stiffness given in the numerical example below, these loads correspond to storey drifts

$$w(\mathrm{T};\ \mathrm{q}=1.0) = \frac{34.6\ \mathrm{kN}\cdot 1.5}{1.0995\ \mathrm{kN/mm}} = 47.2\ \mathrm{mm} \tag{29}$$

$$w(\mathrm{T};\ \mathrm{q} = 1.5) = \frac{34.6\ \mathrm{kN}}{1.0995\ \mathrm{kN/mm}} = 31.5\ \mathrm{mm} \tag{30}$$

$$w(\mathrm{T};\ \mathrm{q} = 4) = \frac{23.0\ \mathrm{kN}}{1.0995\ \mathrm{kN/mm}} = 20.9\ \mathrm{mm} \tag{31}$$

$$w(\mathrm{T};\ \mathrm{q} = 4) = \frac{13.0\ \mathrm{kN}}{1.0995\ \mathrm{kN/mm}} = 11.8\ \mathrm{mm} \tag{32}$$

Shown above we demonstrated the evolution of the key-figures in a hand-calculation. If the structure under consideration was purely elastic, the chosen seismic event would have caused a maximum storey drift of 47.2 mm, corresponding to a base shear of 34.6 kN · 1.5 = 51.9 kN. If we omit the limit condition given in eq. 18 as being arbitrarily man-made rather than being a physical description of a SDOF oscillator under seismic loads, we end up with a storey drift of 11.8 mm acc. eq. 32 instead of 20.9 mm acc. eq. 31. As should be for a structure with an assumed behaviour factor of q = 4, the dissipative storey drift is by a factor of 47.2 mm / 11.8 mm = 4.0 smaller than the elastic storey drift.

As a summary for this section we can conclude, that the structure used in the numerical study is well designed seismic loads given by the lateral force method. Assuming a behaviour factor of q = 4, which is not unusual for a steel sway frame, we receive a horizontal storey load of 23.0 kN, while the structure has a horizontal elastic limit load of 57.6 kN, leading to a utilization of η = 23.0 kN / 57.6 kN = 0.40. *Knoedel/Hrabowski* suggest a modification of the behaviour factor, if the utilization is lower than 0.70 ([4] eq. 27). For the present example, this would lead to

$$q_{mod} = \eta \cdot \mathrm{q} = 0.4 \cdot 4.0 = 1.6 \tag{33}$$

But still, as we can see from eq. 24, with a reduced behaviour factor of app. 1.5 the structure receives a lateral force of 34.6 kN, so that the utilization is η = 34.6 kN / 57.6 kN = 0.60. Another modification of the behaviour factor would lead to q = 1, where the lateral force is 51.9 kN and the final utilization is η = 51.9 kN / 57.6 kN = 0.90. So, under all considerations the structure does meet the requirements of the lateral force method.

After the very explicit evaluation of the numbers given above the effects of mass variation (half and double) are given in Table 1.

Quantity	Unit	36 t q = 1.5	36 t q = 4	72 t q = 1.5	72 t q = 4	144 t q = 1.5	144 t q = 4
plateau base shear F_b	kN	144	54	288	108	576	216
fundamental period T	s	1.14		1.61		2.27	
frequ. red. factor k	–	0.22		0.12		0.058	
base shear $F_b(T)$	kN	31.7	11.9	34.6	13.0	33.4	12.5
storey drift	mm	28.8	10.8	31.5	11.8	30.4	11.4
lower bond condition	kN		23.0		23.0		23.0
storey drift	mm		20.9		20.9		20.9

Table 1. Results of mass variation with lateral force method

We can summarize, that the plateau base shear increases proportional to an increasing mass. If the fundamental period $T_B \leq T \leq T_C$. For other configurations, the horizontal acceleration is lower than the plateau value according to the shape of the response spectrum. Period or frequency are influenced under-proportional by the mass, see eq. 3. However, multiplying the mass with the acceleration, higher mass leads to higher base shear in all cases [14].

3.4 Pushover Analysis

In EC8 [2], the non-linear (quasi-)static pushover analysis is named in Clause 4.3.3.1 (4c). Advantage of the pushover analysis is, that a sequence of different plastic mechanisms can be activated in design (e.g. for a ten storey building in [19]).

Within the frame of the below numerical study also several pushover analyses were provided, see Table 2.

material constitutive law	gravity + second order effects	ultimate horizontal force (FEA) [kN]	ultimate storey drift (FEA) [mm]	ultimate plastic strain (FEA) [%]
elastic	yes	> 173	> 249	0 (Run_30)
plastic	yes	32.1	59	0 (Run_29)
plastic	no	71.1	72	1.14 (Run_28/31)
elastic	no	> 150	> 138	0 (Run_27)

Table 2. Results of various pushover analyses [20]

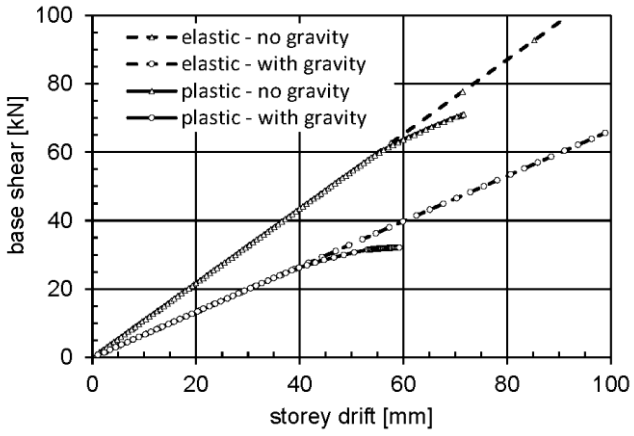

Fig. 6. Load-displacement paths of various pushover analyses with 72 t storey mass

It should be noted, that a storey mass of 72 t would be distributed to much more columns than 2 in a real structure, so the loading of an individual column would be much lower, if the whole building structure was modelled and not only the bracing system. On the other hand, the P-Δ-effect remains the same, independent of how many sway-columns are involved.

Useful hints for practical application are given in [21].

4 NUMERICAL STUDY

4.1 Model

Geometry

The results of [5], with a background documentation given in [6] and the results of [8] with a background documentation given in [9] are used as a basis for the present study. A more extensive background documentation on the present study is given in [20].

Size of frame: 6 m wide, 4 m high; pinned bases, rigid corners; weightless;
Cross sections: Tubular 1000x12 as waler; tubular 240x12 as columns;

Masses

36 000 kgs in each corner of the frame, giving a total storey mass of 72 000 kgs.

Element

BEAM23; 5 integration layers at 50 %; 30 % and 0 % of the beam's height.

Material

Steel with a simplified bi-linear constitutive law and isotropic hardening was used. Isotropic hardening was chosen in order to get symmetrical response amplitudes, although this does not seem to be a proper choice for structural steels or aluminium [10], [22].

Young's modulus with 210 GPa is used up to a yield limit of 235 MPa. Above that a straight line to the ultimate tensile stress 360 MPa at assumed 20 % strain was used. Thus an *engineering plastic modulus* with a slope of

$$E_{tan,plast} = \frac{f_u - f_y}{\varepsilon_u - \varepsilon_y} = \frac{360\ MPa - 235\ MPa}{0.2000 - 0.0011} \approx 625\ \text{MPa} \tag{34}$$

is received, which corresponds to 0.3 % of *Young*'s modulus. This approach has been used before, see eq. 15 in *Knoedel/Hrabowski* (2012) [4].

Remark: In this case material degradation is not considered, therefore accumulated plastic strain is not recorded [23].

Verification

Quantity	Unit	DBF design by formulae	FEA	relative error of FEA [%]
storey drift stiffness	N/m	$1.0995 \cdot 10^6$	$1.0868 \cdot 10^6$	–1.16
horizontal elastic limit force	kN	57.6	56..4	–2.08
horizontal elastic limit drift	mm	52.4	51.9	–0.95
fundamental period	s	1.6075	1.6172	+0.60
fundamental period with half masses	s	1.1368	1.1432	+0.56
fundamental period with double masses	s	2.2733	2.2872	+0.61

Table 3. Comparison of „hand" and FEA results

The performance of the model was tested in various static and time-history runs. The results are given in Table 3.

4.2 Procedure

Time history runs were performed. A horizontal motion was prescribed at the column bases, typically ±50 mm with 1.6170 s as driving period. 200 load steps were used within one period, having 10 to 100 prescribed subdivisions of each individual load step.

This 50 mm amplitude is slightly less than the elastic limit storey drift. But if material non-linearity is switched off, the frame has a storey drift of 78 mm in the first response peak. Thus plastic action starts within the first half wave.

4.3 Results

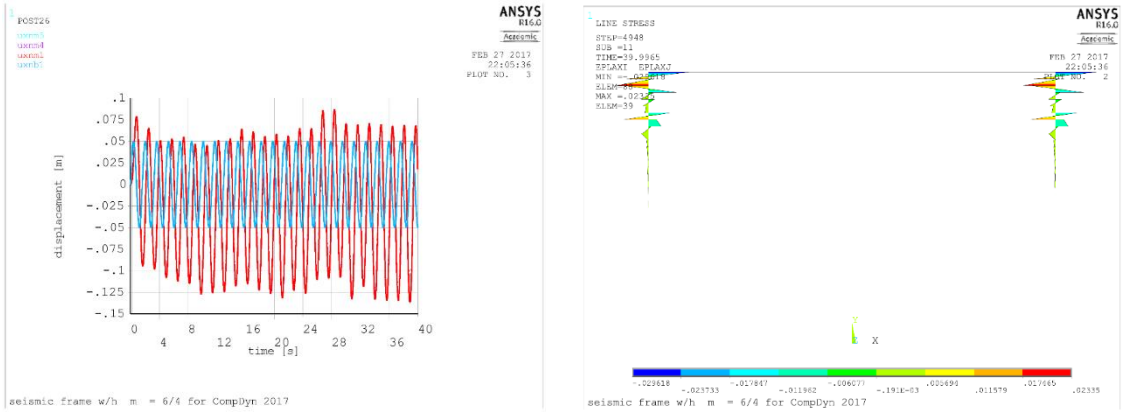

Fig. 7. Exemplary results of run_10 [20]:
a) time history of displacements – drive (blue) and response (red); b) plastic strains at 40 s

In Fig. 7a a typical time history plot is given. We see discontinuous jumps of the response amplitude at continuous harmonic drive, which can not be explained at the moment. The choice of a isotropic hardening constitutive law should provide increasing amplitudes with increasing number of cycles. However, these discontinuities or offset has been observed in a previous study as well, see [8] Fig. 6. We want to investigate this effect in a subsequent study [24].

In Table 4 some key-results of the time history analyses are given. DAF+, DAF– and DAF,range indicate the biggest positive response peak, the biggest negative response peak and half of the biggest range. The run number is referring to the background document [20]. A graphical representation is given in Fig. 8. The numbers in the DAF index are the driving amplitudes.

Initial hypothesis of this paper was, that mass and dissipation are counterparts in order to avoid excessive response displacements. In this study, the structure has a given ability for dissipating energy, i.e. two columns which can develop plastic zones, if the elastic limit storey drift is exceeded. Thus, we should expect that bigger masses are associated with bigger response amplitudes. The response amplitudes are normalized by the driving amplitude, resulting in the dynamic amplification factor DAF. Therefore, all the curves in Fig. 8 should rise from left to right. As we can see, this holds for the negative peaks DAF–, which are marked by a triangle. Some of the other lines are horizontal, some are falling.

Seen from the displacement time history in Fig. 7a and the other ones documented in [20] it seems, that DAF,range is a more reliable indicator of the structure's performance than DAF+ or DAF–, although it does not represent the real maximum of the displacements. On the other hand, since the structure develops plastic zones anyway, it does not seem very significant if the structure has single peaks with bigger amplitudes. A more extensive discussion on limit plastic strains with FEA can be found in [25] and [26].

As we can see from displacement time history of Run_9 [20] after 10 sec we have an elastic response amplitude of app. 900 mm (7. peak). Thus, a structure with a behaviour factor of q = 4 would be having maximum amplitudes of 900 mm / 4 = 225 mm, which would correspond to a DAF = 225 mm / 50 mm = 4.5. As we see from Fig. 8, this condition is met for the structure with 72 t and 50 mm drive.

Run no.	driving amplitude	storey mass	DAF+	DAF–	DAF,range	ζ_{eff} from DAF,range see eq. 6
[-]	[mm]	[t]	[-]	[-]	[-]	[-]
16	25	36	5.89	3.12	3.55	0.14
15	50	36	1.75	2.44	2.09	0.24
17	100	36	2.22	3.53	4.54	0.11
11	25	72	5.07	3.13	3.54	0.14
10	50	72	1.74	2.73	2.05	0.24
12	100	72	3.63	4.72	2.78	0.18
22	25	144	3.73	5.14	3.54	0.14
20	50	144	1.58	4.17	2.09	0.24
21	100	144	3.37	5.14	3.54	0.14

Table 4. Results of the time history analysis

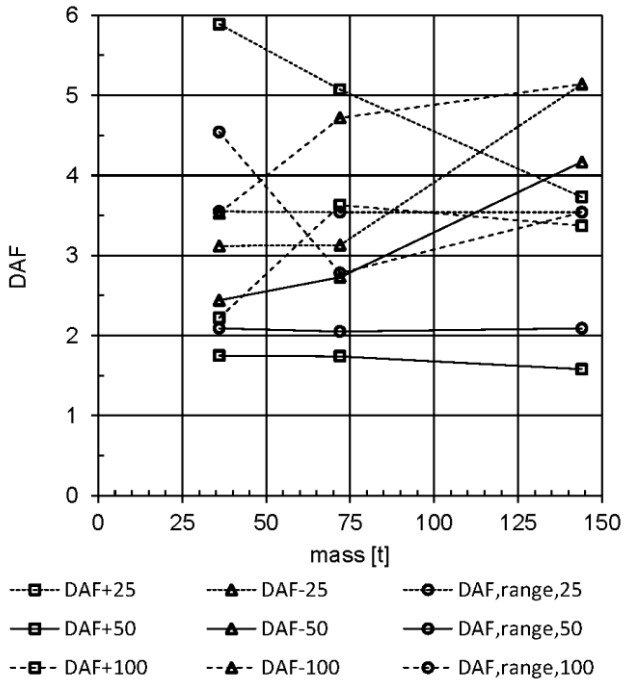

Fig. 8. DAF vs. mass in time history analysis

In the last column of Table 4 we interpreted the dissipative (plastic) action of the structure as viscous damping and evaluated a damping ratio from DAF,range according to eq. 6. Under the assumption of elastic structures having a damping ratio of 5 % in EC8 and a behaviour factor of q = 4 for this kind of frame, these values should coincide with an effective damping ratio of $0.05 \cdot 4 = 0.20$. As we see, this condition is met the configurations with a driving amplitude of 50 mm.

For driving amplitudes 25 mm we have smaller damping. Since 25 mm is only half of the elastic limit amplitude, this configuration could be interpreted as having a utilization of come

50 %. Based on [4], in this case we should reduce the behaviour factor to half, so that the expected damping ratio would be $0.05 \cdot 4 / 2 = 0.10$, which is met.

For driving amplitudes 100 mm we have smaller damping as well. In comparison with 50 mm driving amplitude, this could be interpreted as the structure having insufficient plastic "abilities" for the present mass. As a result additional damping devices would be needed, which could be a third column in this simple example.

5 CONCLUSIONS

- Time history analysis with harmonic drive is preferred by the authors when studying basic correlations, because according to Table 1 in [8] this is the last level where you can make plausibility checks.
- It is very difficult, to adapt an artificial base drive such, that results are achieved, which can be proved to be in line with the provisions of EC8. Basically, this difficulty results from the fact, that quasi-static methods can not simulate dynamic problems.
- Pushover analysis has the advantage, that it can be performed at low effort.
  However, since it is a quasi-static method, it needs to be based on assumptions on the magnitude of the horizontal inertial forces. Typically, these assumptions are based on the evaluation of the response spectrum of a SDOF oscillator. As a consequence, it is difficult to use this method for multi-storey buildings, if higher modes than the fundamental one are governing.
- Within the lateral force method, variation of masses leads to proportional variation of the base shear, if the fundamental period is within the plateau of the response spectrum. In other cases the variation of the base shear is non-proportional, but in all cases increased mass leads to increased base shear.
- This behaviour can not be captured in all cases by a time history analysis with different driving amplitudes. We found configurations, where increasing masses produced decreasing response amplitudes.
- Some of the features we found in our study are inconsistent and need further work, such as non-increasing amplitudes with isotropic hardening and sudden offsets in the response amplitudes.
- So far, we found no evidence to exclude a viscous-damping-approach for plastic structures. That is at least within the range of accuracy needed in seismic design according to EC8.

6 ACKNOWLEDGEMENT

The continuous support of Dipl.-Ing. Tobias Wacker, ANAKON Karlsruhe, is greatfully acknowledged. The authors are indebted to Dr Evangelos Efthymiou, Aristotle University of Thessaloniki and Prof. Bogdan Stefanescu, Technical University of Bucharest, for fruitful discussions.

REFERENCES

[1] EN 13445: Unfired pressure vessels.
Part 1: General, 2014.

Part 3: Design, 2009.
Amendment A1, August 2012; Draft Amendment A2, July 2012.

[2] EN 1998 (EC8): Design of structures for earthquake resistance.
Part 1: General rules, seismic actions and rules for buildings:2004 + AC:2009 + A1:2013.

[3] Knoedel, P.: On the Dynamics of Steel Structures with X-Type Bracing.
Stahlbau 80 (2011), No. 8, p. 566–571.

[4] Knoedel, P., Hrabowski, J.: Yield Limit vs. Behaviour Factor in Seismic Design. Proceedings, NSCC 2012 Nordic Steel Construction Conference, 5-7 September 2012, Oslo, Norway, pp 147-155.

[5] Knoedel, P., Hrabowski, J., Ummenhofer, T.: Seismic behaviour factor in combined frame and braced structures. Eurosteel 2014, 7th European conference on steel and composite structures, Naples, Italy, 10-12 September 2014. (see [6])

[6] Knoedel, P. "Background document on ANSYS analyses" 09.03.2014, to be downloaded from http://www.peterknoedel.de/lehre/FHA-Stahl/Skript/GrA/Dyn/report-11_14-03-09.pdf, see [5]

[7] Knödel, P., Heß, A.: Erdbebenbemessung von Tanks – Erfahrungen aus der Praxis. Stahlbau 80 (2011), Heft 11, S. 820–827. (Seismic design of tanks – practical experience)

[8] Knoedel, P., Ummenhofer, T.: Time History Simulation in Seismic Design. Contribution 379 (USB). Heinisuo, M., Mäkinen, J. (eds).: Proceedings, NSCC-2015 Nordic Steel Construction Conference 2015, Tampere, Finland, 23-25 September 2015. (see [9])

[9] Knoedel, P. "NSCC 2015 - Background document on ANSYS analyses" 10.02.2015, to be downloaded from http://http://www.peterknoedel.de/lehre/FHA-Stahl/Skript/GrA/Dyn/report-07_15-02-10.pdf, see [8]

[10] Efthymiou, E., Psomiadis, V.G., Ampatzis, A.T.: Aluminium Deployment in Bracing Systems: Investigation of Shear Link Application. Contribution 371 (USB). Heinisuo, M., Mäkinen, J. (eds).: Proceedings, NSCC-2015 Nordic Steel Construction Conference 2015, Tampere, Finland, 23-25 September 2015.

[11] Li, A., Gao, R., Sun, M., Zhang, J.: Research on hysteretic behaviours of a separated shock absorber applied in railway bridge. Papadrakakis, M., Papadopoulos, V., Stefanou, G., Plevris, V. (eds.): Proc. ECCOMAS 2017, VII Europ. Congress on Comp. Meth. in Appl. Sci. and Eng., 05-10 June 2016, Crete Island, Greece.

[12] Öniz, S.: Dissipative Stahlblechverbindungen für Brettsperrholz unter wiederholter zyklischer Belastung. Dissipative steel plate connections for CLT under repeated cyclic stress. Master Thesis at KIT Timber Structures and Building Construction, Karlsruhe 2016.

[13] Sandhaas, C., Schädle, P.: Joint properties and earthquake behaviour of buildings made from dowel-laminated timber. Paper No 3379 in Proc., 16WCEE 2017, 16th World Conference on Earthquake Engineering, 09.-13.01.2017, Santiago de Chile.

[14] Mueller, A., Knoedel, P., Koelle, B.: Critical Filling Levels of Silos and Bunkers in Seismic Design. Paper no. 0464, Proc., 15 WCEE 15th World Congress on Earthquake Engineering, Lisbon 24-28.09.2012.

[15] Knoedel, P.: Lecture notes on Steel Construction at the University of Applied Sciences Augsburg, Germany. To be downloaded from

www.peterknoedel.de/lehre/lehre.htm, updated regularly from March 2007 to March 2013. Dynamik – Grundlagen (lineare Schwinger) (Dynamics – Basics – linear oscillators)

[16] Duffing, G.: Erzwungene Schwingungen bei veränderlicher Eigenfrequenz und ihre technische Bedeutung. Sammlung Vieweg Heft 41/42, Braunschweig 1918. (cited after [17])

[17] Petersen, Chr.: Dynamik der Baukonstruktionen. Vieweg, Wiesbaden, 1996.

[18] Nagel, S.: Studies on the Seismic Design of Network Arch Road Bridges. Master Thesis at KIT Steel and Lightweight Structures, Karlsruhe 2015.

[19] Köber, H., Stoian, M., Stefanescu, B.C.: Different Bracing Types in Seismic Resistant Structures. Paper 20-602 in EuroSteel 2014, 7th EUROpean conference on STEEL and Composite Structures, Naples, Italy, 10-12 September 2014.

[20] Knoedel, P. "Knoedel/Ummenhofer at Eurosteel Copenhagen; Mass Variation with dissipative Steel Structures under Seismic Loads; Background Document on FE Study" 12.03.2017, to be downloaded from http://www.peterknoedel.de/lehre/FHA-Stahl/Skript/GrA/Dyn/report-11_17-03-12.pdf.

[21] FEMA 440: Improvement of Nonlinear Static Seismic Analysis Procedures. Prepared by ATC Applied Technology Council (ATC-55 Project), Redwood City, California. Prepared for Dept. Homeland Security, Federal Emergency Management Agency, Washington D.C., June 2005.

[22] Gkatzogiannis, S., Knoedel, P., Ummenhofer, T.: FE welding residual stress simulation: Influence of boundary conditions and material models. Submitted to Eurosteel 2017, 8th European Conf. on Steel and Composite Structures. 15-17 September 2017, Copenhagen, Denmark. Paper no. 483 (submitted).

[23] Tappauf, C., Taras, A.: Deformation and Strain Histories in Shell-to-Base Joints of Unanchored Steel Storage-Tanks during Seismic Loading. 8th Int. Conf. on Behavior of Steel Structures in Seismic Areas, Shanghai, China, July 1-3, 2015.

[24] Knoedel, P., Nagel, S., Ummenhofer, T.: From 3-D time history simulation to lateral force method – a study on hand design rules. (in preparation)

[25] Knödel, P., Ummenhofer, T.: Regeln für die Berechnung von Behältern mit der FEM. Stahlbau 86 (2017), Heft 4. (Rules for calculating tanks and silos with FEM, in print)

[26] Knödel, P., Ummenhofer, T., Ruckenbrod, C.: Silos und Tanks. Kuhlmann, U. (ed.): Stahlbau-Kalender 2017, Ernst & Sohn, Berlin (in print).